Bifurcation delay in a network of locally coupled slow-fast systems

D. Premraj,[1] K. Suresh,[2] Tanmoy Banerjee,[3] and K. Thamilmaran[1]
[1]*Centre for Nonlinear Dynamics, School of Physics, Bharathidasan University, Tiruchirappalli-620 024, Tamil Nadu, India*
[2]*Department of Physics & Astrophysics, University of Delhi, Delhi-110007, India*
[3]*Chaos and Complex Systems Research Laboratory, Department of Physics, University of Burdwan, Burdwan 713 104, West Bengal, India*

(Received 14 March 2018; revised manuscript received 8 July 2018; published 8 August 2018)

We study the evolution of bifurcation delay in a network of locally coupled slow-fast systems. Our study reveals that a tiny perturbation even in a single node causes asymmetry in bifurcation delay. We investigate the evolution of bifurcation delay as a function of various parameters, such as feedback coupling strength, amplitude of external force, frequency of external force, and delay coupling strength. We show that a traveling wave is generated as the result of introducing local parameter mismatch, and the bifurcation delay shows a dip in the spatial profile. We believe that these spatiotemporal patterns in bifurcation delay shed light on the dynamics of neuronal networks.

DOI: 10.1103/PhysRevE.98.022206

I. INTRODUCTION

Many physical systems evolving with multiple time scales can be modeled as fast and slow systems [1–4]. In such systems, parameters may vary slowly with time or they can be deliberately varied by the researcher. For instance, the weight of a rocket in flight slowly decreases due to the burning of fuel, which improves the speed of the rocket [5,6]. Catalytic activities in chemical reactors slowly decline due to chemical erosion and decrease the reactor performance [7,8]. The time dependence of a parameter may cause dramatic changes in the bifurcation diagram, which is obtained under the assumption of a stationary control parameter. One special feature of slow and fast systems is that bifurcation does not happen immediately at the bifurcation point as a result of the slow state variable regarded as the bifurcation parameter. These dynamical phenomena are called delayed bifurcations or the slow passage effect, which are of interest for their importance in applications to various scientific fields including experiments with lasers [9], fluid convection [10], electronic circuits [11], and bistable chemical reaction [12,13].

Delayed bifurcation was first reported in the study of Hopf bifurcation of a slow-fast system by Shishkova [14]. Delay behaviors can also be observed in ordinary differential equations with slowly varying parameters, such as the slow passage problem through Hopf bifurcations [8], pitchfork bifurcations [15], saddle-center bifurcations [16], transcritical bifurcations [17], and through the resonances [18,19]. Such a phenomenon is also observed in parametrically driven systems in which the system is driven by a single or two periodic forces while the control of bifurcation delay is also studied for the influence of self-feedback delay [20–22]. In particular, Baer *et al.* [8] have studied the bifurcation delays in the FitzHugh-Nagumo model of nerve membrane excitability. It was shown that bifurcation delays in the onset of oscillations due to the slow passage effect decrease due to the influence of small-amplitude noise and periodic environmental perturbations of near-resonant frequency. Whereas many of the studies related to the bifurcation delay problem have focused on a single system, in this work we address the question of how the bifurcation delay evolves in a network of slow-fast systems that are coupled through their nearest neighbors.

Generally networks of coupled oscillators exhibit diverse collective behaviors, such as synchronization, traveling waves, clustering, and chimera states depending on the interplay of coupling and local dynamics [23]. All of these phenomena are manifested in phase, amplitude, or both [24–26]. However, the manifestation of coupled behaviors in the context of bifurcation delay has not been studied in the past. In the present study, we investigate the evolution of bifurcation delay in a network of locally coupled FitzHugh-Nagumo oscillators, which are paradigmatic oscillators in the field of biology and neuroscience that show slow-fast dynamics. Here we focus on the dynamics under local coupling as it often arises in neuronal systems [27], fluid dynamics [28], and chemical oscillations [29].

In the present study, we show that even a tiny perturbation in the parameters of a single node of a network of locally coupled slow-fast systems leads to asymmetry in bifurcation delay and also causes various spatiotemporal patterns, such as traveling-wave and synchronized states. In the case of a traveling wave, the bifurcation delay shows a dip in the spatial profile. We analyze the behavior of the bifurcation delay under various parametric conditions, such as the variation in coupling strength, amplitude, and frequency of perturbation and variation in delays.

The rest of the paper is organized as follows: In Sec. II we introduce the model of a locally coupled network of FitzHugh-Nagumo (FHN) systems. Then we demonstrate the bifurcation delay in a network of identical FHN systems in Sec. III. The effect of bifurcation delay under single-node perturbation is discussed in Sec. IV. Finally, we summarize our results in Sec. V.

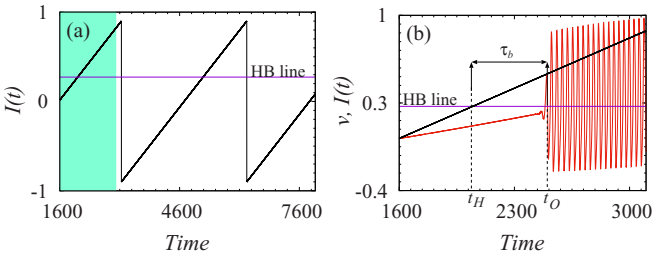

FIG. 1. (a) Time-varying current $I(t)$ given by Eq. (2). The shaded region corresponds to the $I(t)$ value for which (b) is plotted. (b) Time evolution of the activator variable v for a single FitzHugh-Nagumo system. The solid black line represents (increasing) $I(t)$. Here $\tau_b = t_O - t_H$ is the bifurcation delay time. The HB line is the Hopf bifurcation line, which is the boundary between the oscillatory region and the steady-state region.

II. NETWORK OF LOCALLY COUPLED FITZHUGH-NAGUMO SYSTEMS

We consider a network of N locally coupled FitzHugh-Nagumo (FHN) systems given by

$$\begin{aligned}\dot{v}_j &= -h(v_j(t)) - w_j(t) + I(t) + \varepsilon[v_{j-1}(t-\tau) - v_j(t)] \\ &\quad + \varepsilon_f v_j(t-\tau_f), \\ \dot{w}_j &= b[v_j(t) - f w_j(t)]. \end{aligned} \tag{1}$$

Here $h(v_j(t)) = v_j(t)[v_j(t) - a][v_j(t) - 1]$, and v and w are the activator and inhibitor variables, respectively. $a, b, f > 0$ are system parameters. A node index represented by j ($j = 1, 2, \ldots, N$) is taken as modulo N, i.e., we consider a periodic boundary condition. Coupling delay is represented by τ and self-feedback delay is given by τ_f. These two types of delays have different origins in the context of a realistic neuronal system: self-feedback delay (τ_f) arises due to the finite processing time with which the neural system responds to a stimulus, whereas coupling delay (τ) comes into play due to the finite time of propagation of an information signal between the spatially separated neurons [30,31]. Therefore, it is important to study the simultaneous impact of both kinds of delays. Here ε represents the strength of the delayed coupling, and ε_f is the self-feedback coupling strength. The slowly varying *injection current* $I(t)$ in Eq. (1) is represented by

$$I(t) = \frac{-3\alpha}{\pi}[\tan^{-1}(\cot(\omega_j t))]. \tag{2}$$

The rate of variation of $I(t)$ corresponding to the jth oscillator is controlled by ω_j, whereas α controls the amplitude. Note that the particular form of $I(t)$ given by Eq. (2) represents a sawtooth function [see Fig. 1(a)] that enables one to consider a slow linearly increasing variation of $I(t)$ in a cycle. In the absence of the time-varying current $I(t)$, the system (1) resides in the excitable state [8]. A proper value of $I(t)$ drives the system to the oscillatory mode through Hopf bifurcation.

To study the evolution of bifurcation delay, we consider the following parameter values throughout the paper: $a = 0.2$, $b = 0.05$, and $f = 0.4$. Parameters for injection current $I(t)$ are $\alpha = 0.8$, $\omega_j = 0.001$; note that we choose a small value of ω_j to make the injection current a slowly varying function.

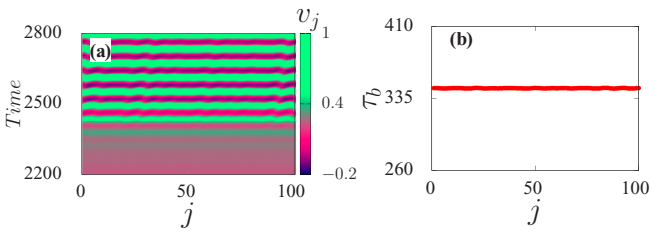

FIG. 2. (a) Spatiotemporal plot taken by considering the identical system that is $\omega_j = 0.001$, where $j = 1, 2, 3, \ldots, N$, and (b) their corresponding bifurcation delay in the system. Other parameter values: $a = 0.2$, $b = 0.05$, $\alpha = 0.8$, $f = 0.4$, $\tau_f = 11$, $\tau = 9$, $\varepsilon = 0.2$, and $\varepsilon_f = 0.2$.

Now let us consider a single FitzHugh-Nagumo oscillator [i.e., Eq. (1) with $j = 1$, $\varepsilon = 0$, and $\varepsilon_f = 0$]. With the variation of the external current $I(t)$, the appearance of bifurcation delay is shown in Fig. 1(b) for illustrative purposes. The HB line represents the Hopf bifurcation line, which is the boundary between the steady-state and the oscillatory region. The delay in transition from the excitable state to the oscillatory state, denoted by τ_b, is observed by comparing the time t_O at which the system oscillates [t_O is marked where the oscillation reaches 1/10 of the maximum amplitude of $v_j(t)$] and the time t_H when $I(t)$ crosses the Hopf bifurcation line. Hence the delay τ_b is calculated as $\tau_b = t_O - t_H$. The detailed quantitative analysis of bifurcation delay for a single system was given by Baer *et al.* [8]; they showed that the delay associated with the bifurcation can be attributed to the fact that the destabilization of the slowly varying solution does not occur immediately. Also note that [see Fig. 1(a)] after the end of the increasing cycle of $I(t)$, it suddenly jumps below the HB line, and the oscillation in $v(t)$ will cease (not shown in the figure). Here the system again enters into the excitable state, and the whole cycle repeats itself.

III. BIFURCATION DELAY IN A NETWORK OF IDENTICAL FHN SYSTEMS

Before we discuss the results of the network under local parameter mismatch, to understand the scenario in a better way we discuss the phenomenon of bifurcation delay in a network of *identical* FitzHugh-Nagumo systems. For this we consider 100 FHN systems, and each oscillator is coupled through nearest-neighbor coupling obeying Eq. (1). Numerical integration is carried out using a fourth-order Runge-Kutta algorithm with a step size 0.001. Coupling parameters are $\tau = 9$, $\tau_f = 11$, $\varepsilon = 0.2$, and $\varepsilon_f = 0.2$. If all the oscillators are identical to the above-mentioned parameters, they all experience the same bifurcation delay. This can be seen from Fig. 2, where all 100 oscillators show a coherent spatiotemporal profile of v_j [Fig. 2(a)], and Fig. 2(b) shows the magnitude of the bifurcation delay (τ_b), which is the same for all the oscillators.

IV. BIFURCATION DELAY UNDER SINGLE-NODE PERTURBATION

In this section, we numerically explore the behavior of bifurcation delay τ_b when any one of the representative oscillators (say the oscillator with index $j = 10$) is different from other

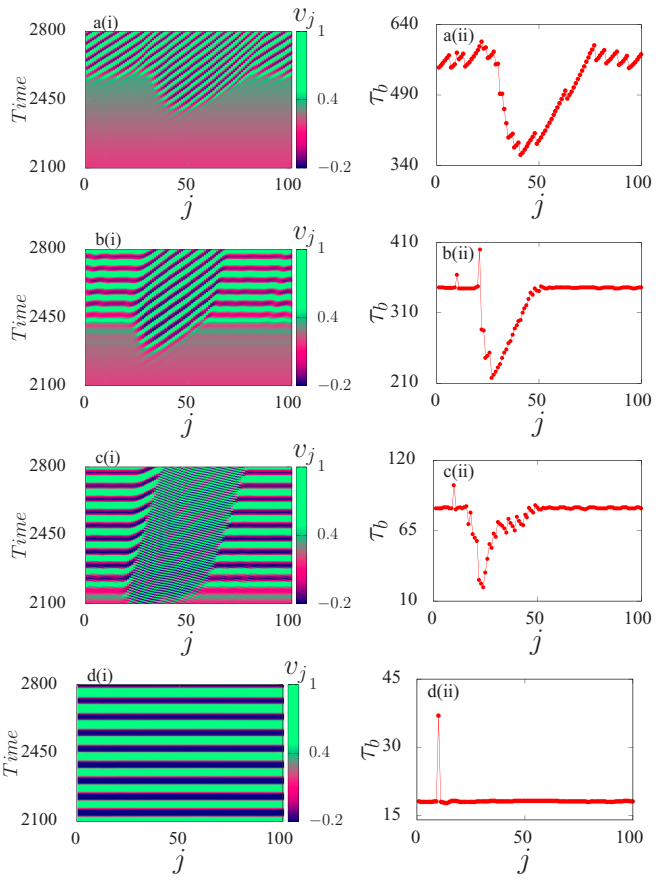

FIG. 3. Spatiotemporal plots (left panels) and bifurcation delay (right panel) under the perturbation in the 10th oscillator with $\omega_{10} = 0.001\,01$: (a) (i-ii) traveling-wave state having incoherent bifurcation delay for $\varepsilon_f = 0.1$. (b) (i-ii) and (c) (i-ii): Spatiotemporal plots show mixed states of synchronized and TW patterns having constant as well as different bifurcation delay for $\varepsilon_f = 0.2$ and 0.3, respectively. (d) (i-ii) Synchronized state for $\varepsilon_f = 0.5$; here bifurcation delay of all the oscillators is equal except for the perturbed node. Other parameter values: $a = 0.2$, $b = 0.05$, $\alpha = 0.8$, $f = 0.4$, $\tau_f = 11$, $\tau = 9$, $\varepsilon = 0.2$, and $\omega_j = 0.001$ (except $j = 10$).

oscillators. We choose the value of frequency of the current $I(t)$ of the 10th oscillator as $\omega_{10} = 0.001\,01$, which is different from that of the rest of the oscillators, $\omega_j = 0.001$ ($j \neq 10$). We verify that because of the periodic boundary condition, the choice of the perturbed node is arbitrary and does not affect our results. Note that here the local parameter mismatch in frequency is indeed tiny and constant. In the following subsections, we will investigate the behavior of bifurcation delay τ_b under various parametric conditions, namely the variation in self-feedback coupling strength, the amplitude of the external current, the frequency of the external current, the variation in the delay coupling strength, and the effect of coupling delay and self-feedback delay.

A. Variation of bifurcation delay with feedback coupling strength ε_f

To explore the effect of ε_f on the bifurcation delay, we fix the delay-coupling strength at $\varepsilon = 0.2$. By varying the feedback coupling strength ε_f, one can observe different

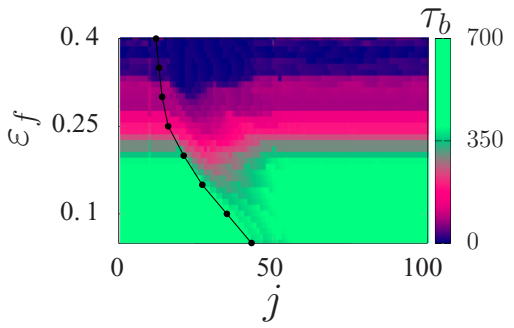

FIG. 4. Bifurcation delay for the system of oscillators as a function of ε_f for a fixed $\varepsilon = 0.2$. The line points show how the index of the leftmost oscillator of the disparate region (or dipping region) shifts spatially with the variation of ε_f. For other parameters, see the text.

interesting scenarios. For a sufficiently small value of $\varepsilon_f = 0.1$, we observe that the system of oscillators exhibits traveling waves [shown in Fig. 3(a)(i)]. The bifurcation delay associated with Hopf bifurcation is illustrated in Fig. 3(a)(ii): It can be seen from the figure that the bifurcation delay of each oscillator is disparately distributed, and it shows a dip around $j = 50$. Interestingly, we find that this dip in τ_b is related to the traveling nature of v_j. It can be revealed by increasing the value of ε_f to $\varepsilon_f = 0.2$: now the system of oscillators splits into two groups: one group has a synchronized v_j profile, and in the other group v_j shows a traveling wave (TW) [Fig. 3(b)(i)]. The corresponding bifurcation delay is demonstrated in Fig. 3(b)(ii): it clearly shows that in the synchronized domains, oscillators have almost the same bifurcation delay (except the perturbed node), while in the TW domain a sudden dip in τ_b is observed. A similar behavior can also be observed for $\varepsilon_f = 0.3$, which is shown with Figs. 3(c)(i) and 3(c)(ii), however we note that an increasing ε_f increases the traveling speed, and with increasing traveling speed the depth of the dip decreases. By further strengthening the feedback coupling strength, the magnitude of bifurcation delay τ_b decreases and all the oscillators are now synchronized and have the same bifurcation delay except for the node $j = 10$, which is perturbed by introducing a frequency mismatch with other nodes [see Figs. 3(d)(i) and 3(d)(ii)].

Further, the variation of bifurcation delay as a function of ε_f is investigated in more detail for a fixed $\varepsilon = 0.2$; the results are presented in Fig. 4. It shows the magnitude of bifurcation delay as a function of ε_f in j-ε_f space. We observe that for smaller values of ε_f the magnitude of bifurcation delay is large, while increasing the value of the coupling strength causes the magnitude of delay to decrease. When ε_f approaches the value 0.4, we can observe that bifurcation delays associated with all the oscillators become constant (except for $j = 10$, i.e., the perturbed node). This may be due to the fact that for stronger self-feedback, the synchronization effect dominates over the delayed bifurcation effect scenario. Another notable observation is that for lower coupling strength, the disparate bifurcation delay occurs in the oscillators that are far away from the perturbed node (i.e., $j = 10$). While ε_f is increased, the number of oscillators in the disparate state increases at the same time that the leftmost oscillator belonging to the disparate

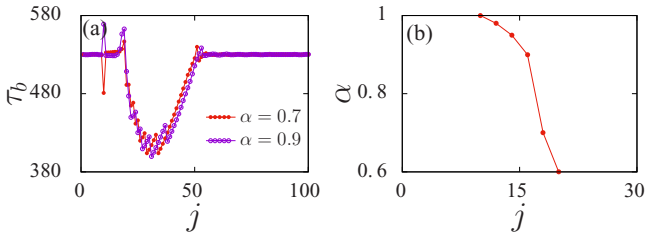

FIG. 5. (a) Bifurcation delay for two different amplitudes with $\alpha = 0.7$ (filled circular points with a solid line), $\alpha = 0.9$ (open circular points with a solid line). Other parameter values: $\tau_f = 11$, $\tau = 9$, $\varepsilon = 0.2$, and $\varepsilon_f = 0.2$. (b) The shift in the index of the leftmost node of the disparate domain with α.

state approaches the perturbed system, and when it reaches the perturbed node the whole network becomes synchronized (the traveling-wave state disappears), which is clearly illustrated in Fig. 4. To show that increasing ε_f leads to a movement of the disparate region toward the perturbed node, we have plotted the index of the leftmost oscillator in the disparate state, which is shown by line points (black filled circles) in Fig. 4. Here, we can see that the spatial shift occurs along the array of the oscillators, and the leftmost oscillator from the disparate state approaches the perturbed system. Our observation of decreasing τ_b with increasing ε_f is consistent with the observation of Ref. [21] by the same authors for a single oscillator, where it was shown that the bifurcation delay is controlled by the interplay of self-feedback delay and propagation delay.

B. Variation of bifurcation delay as a function of the amplitude of $I(t)$

To get an understanding about the impact of the amplitude of the external force, α, on the bifurcation delay (τ_b), we choose two different values: $\alpha = 0.7$ and 0.9. Other parameter values are $a = 0.2$, $b = 0.05$, $\omega_j = 0.001$, $f = 0.4$, $\tau_f = 11$, $\tau = 9$, $\varepsilon = 0.2$, and $\varepsilon_f = 0.2$. From Fig. 5(a), one can note that an increase in amplitude of $I(t)$ does not lead to any qualitative change in the bifurcation delay. Moreover, as in the previous case, an increase in α also leads to a shifting of the leftmost oscillator in the disparate (incoherent) domain toward the perturbed oscillator. This is presented in Fig. 5(b) as a function of α. The line connected by filled circles denotes the index of the leftmost oscillator in the disparate domain, which moves toward the perturbed node (i.e., the 10th oscillator) as α increases.

C. Variation of bifurcation delay as a function of frequency of $I(t)$

Next, we analyze the impact of the frequency of the external force $I(t)$ on the behavior of τ_b. For this, we fix the frequency of the oscillators in the system (except the perturbed node) as $\omega_j = 0.001$. By varying the value of ω_{10} linearly with integral multiples of 0.000 01, that is, $\Delta\omega = k \times 10^{-5}$, $k = 1, 2, 3, \ldots$, we investigate the deviation of τ_b among the system of oscillators. Figure 6(a) illustrates the existence of τ_b for amplitude $\alpha = 0.8$ with fixed $\Delta\omega(\omega_{10} - \omega_j = 0.001\,02 - 0.001) = 0.000\,02$. In the marked region, the bifurcation delay increases linearly with a slope of 4.16. Here we calculated the slope as

$$\text{slope } \Delta\omega = \frac{\tau_b \text{ of oscillator } i - \tau_b \text{ of oscillator } (i-1)}{i - (i-1)}, \quad i \in 21 - 40.$$

The value of this slope increases if we increase $\Delta\omega$. For various $\Delta\omega$, we have plotted their corresponding slope $\Delta\omega$ in Fig. 6(b). For example, if $\Delta\omega = 0.000\,03$, the bifurcation delay between the successive oscillator is 8.7. Figure 6(c) shows a similar slope for two different amplitudes, e.g., for $\alpha = 0.8$ (circular points with a solid line) and $\alpha = 0.9$ (triangular points with a dashed line).

D. Bifurcation delay as a function of delay coupling strength ε

Here, we investigate the behavior of bifurcation delay for fixed self-feedback coupling strength ε_f by varying the delay coupling strength ε. In contrast to the feedback coupling strength ε_f (as in Fig. 4), ε does not qualitatively change the spatial profile of τ_b. Instead, increasing ε spatially shifts the disparate τ_b profile along the array j; this is shown in Fig. 7(a). Another thing to notice here is that with an increase in the coupling strength, shifting occurs away from the perturbed node, while for increasing ε_f shifting occurs toward the perturbed node (see Fig. 4). The line connected by points in Fig. 7(a) clearly delineates the shifting of the index of the leftmost oscillator in the disparate or incoherent domain, which moves away from the perturbed node as ε increases. For illustrative purposes, τ_b of the oscillator for fixed coupling strength ε is plotted in Fig. 7(b). For $\varepsilon = 0.08$ [marked with a horizontal dashed line in Fig. 7(a)], the onset of the disparate or incoherent domain starts at the index $j_d = 15$th oscillator, as shown in Fig. 7(b). If we increase ε, the index j_d spatially moves in the right direction.

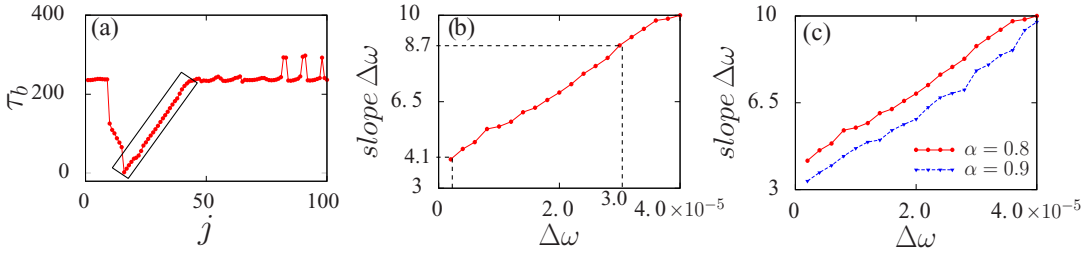

FIG. 6. (a) Bifurcation delay for amplitude $\alpha = 0.8$, $\varepsilon_f = 0.2$, and $\varepsilon = 0.2$ for $\Delta\omega(\omega_{10} - \omega_j) = 0.000\,02$. (b) Slopes for different $\Delta\omega(\omega_{10} - \omega_j)$. (c) Slopes for different $\Delta\omega(\omega_{10} - \omega_j)$ for $\alpha = 0.8$ (circular points with a solid line) and $\alpha = 0.9$ (triangular points with a dashed line).

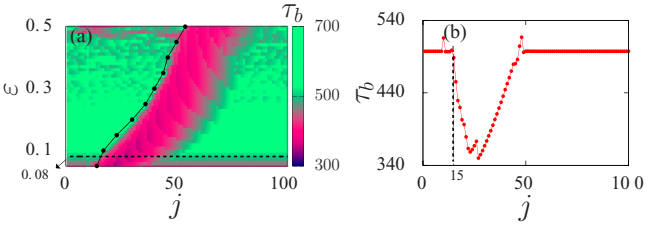

FIG. 7. (a) Bifurcation delay for the system of oscillators as a function of ε for fixed $\varepsilon_f = 0.2$. (b) The bifurcation delay for $\varepsilon = 0.08$ [i.e., bifurcation delay corresponding to the ε value marked with a horizontal dashed line in Fig. 7(a)].

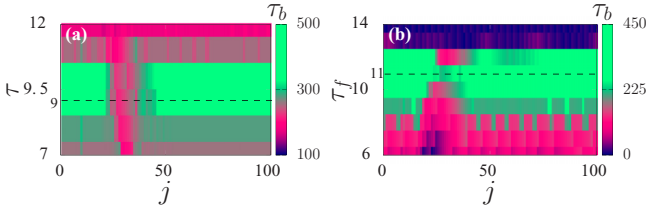

FIG. 8. Bifurcation delay for the system of oscillators as a function of (a) coupling delay (τ) and (b) self-feedback delay (τ_f). The dashed horizontal lines denote selected values of τ and τ_f for the analysis in this paper. Other parameters: $\varepsilon = 0.2$, $\varepsilon_f = 0.2$.

E. Bifurcation delay as a function of coupling delay (τ) and self-feedback delay (τ_f)

Finally, we explore how bifurcation delay changes with the two delay parameters, τ and τ_f. The results of the variation of τ_b with respect to τ and τ_f are shown in Figs. 8(a) and 8(b), respectively. With respect to τ, the coexistence of two domains with different behavior in the region between ($8.5 \leqslant \tau \leqslant 10.5$) is shown in Fig. 8(a) ($\tau_f = 11$): in one domain the system has constant bifurcation delay, while the other has disparate bifurcation delay. Analogously, from Fig. 8(b) one can note that the system exhibits two domains with different bifurcation delay in the region between ($9 \leqslant \tau_f \leqslant 13$) as a function of τ_f ($\tau = 9$). In this paper, we investigate the behavior of bifurcation delay by fixing $\tau = 9$ and $\tau_f = 11$, which are within the regions shown in Figs. 8(a) and 8(b) [shown by a horizontal dashed line in Figs. 8(a) and 8(b)]. However, it would be interesting to explore the behavior of the system in the complete $\tau - \tau_f$ parameter space, which may show much more complex phenomena and would be a potential problem to study.

V. CONCLUSION

In summary, we have investigated the evolution of the bifurcation delay in a network of slow-fast systems under local coupling among the dynamical units. In the case of identical systems, we have found that the profile of bifurcation delay is uniformly distributed along the array of oscillators. However, the introduction of even a very small perturbation at a single node leads to a traveling-wave (TW) state. In the spatial profile of the TW state, bifurcation delay shows a dip in the disparate region. We also analyzed the effect of bifurcation delay with respect to various parameters related to the coupling and external perturbation (here the injection current).

Our numerical study raised the following important open question, which has to be studied in the future: "How does the inhomogeneity created in the system physically govern the evolution of bifurcation delay?" The present study provides an account of the interesting complex behaviors shown by the bifurcation delay in a network of locally coupled slow-fast systems. In this paper, we have chosen the injection current as the source of asymmetry; however, it will be interesting to study the effect of others perturbations, such as noise, and inhomogeneous system and coupling parameters. Further, this study can be extended toward several other coupling topologies, e.g., global coupling and nonlocal coupling. In particular, we believe that under nonlocal coupling, apart from the traveling-wave solution, additional complex patterns such as chimera patterns [24] may emerge, and in this state a separate study is warranted to determine how bifurcation delay evolves. We believe that the present study will shed light on the dynamics of many physical and biological systems in which slow-fast dynamics are present.

ACKNOWLEDGMENTS

The authors are thankful to the anonymous referees for their constructive suggestions. D.P. thanks the University Grants Commission (UGC-RFSMS-BSR), Government of India, for providing support through a research fellowship. K.S. acknowledges support through a UGC-DS-Kothari Post Doctoral Fellowship. K.T. acknowledges support through the Department of Science and Technology (DST-PURSE-Phase-II).

[1] I. T. Georgiou, A. K. Baja, and M. Corless, Int. J. Nonlin. Mech. **33**, 275 (1998).
[2] D. Pieroux and T. Erneux, Phys. Rev. A **53**, 2765 (1996).
[3] R. J. Field and M. Burger, *Oscillations and Traveling Waves in Chemical Systems* (Wiley, New York, 1985).
[4] D. Ludwig, D. D. Jones, and C. S. Holling, J. Anima. Ecol. **47**, 315 (1978).
[5] E. Jakobsson and R. Guttman, Continuous stimulation and threshold of axons: The other legacy of Kenneth Cole, in *The Biophysical Approach to Excitable Systems*, edited by W. J. Adelman and D. E. Goldman (Plenum, New York, 1981), pp. 197–211.
[6] A. I. Neishtadt, Diff. Eqs. **23**, 1385 (1987), Transl. from Diff. Urav. **23**, 2060 (1987).
[7] J. Rinzel and S. M. Baer, Biophys. J. **54**, 551 (1987).
[8] S. M. Baer, T. Erneux, and J. Rinzel, SIAM J. Appl. Math. **49**, 55 (1989).
[9] J. H. Talla Mbé, A. F. Talla, G. R. G. Chengui, A. Coillet, L. Larger, P. Woafo, and Y. K. Chembo, Phys. Rev. E **91**, 012902 (2015).

[10] G. Ahlers, M. C. Cross, P. C. Hohenberg, and S. Safran, J. Fluid Mech. **110**, 297 (1981).
[11] R. Mannella, F. Moss, and P. V. E. McClintock, Phys. Rev. A **35**, 2560 (1987).
[12] J. P. Laplante, T. Erneux, and M. Georgiou, J. Chem. Phys. **94**, 371 (1991).
[13] P. Strizhak and M. Menzinger, J. Chem. Phys. **105**, 10905 (1996).
[14] M. A. Shishkova, Dokl. Akad. Nauk SSSR **209**, 576 (1973).
[15] R. Haberman, SIAM J. Appl. Math. **62**, 488 (2001).
[16] D. C. Diminnie and R. Haberman, Physica D **162**, 34 (2002).
[17] X. Han, Q. Bi, C. Zhang, and Y. Yu, Int. J. Bifurcation Chaos **24**, 1450098 (2014).
[18] L. Ng, R. Rand, and M. O'Neil, J. Vib. Control. **9**, 685 (2003).
[19] Y. Park, Y. Do, and J. M. Lopez, Phys. Rev. E **84**, 056604 (2011).
[20] D. Premraj, K. Suresh, T. Banerjee, and K. Thamilmaran, Commun. Nonlin. Sci. Numer. Simulat. **37**, 212 (2016).
[21] D. Premraj, K. Suresh, T. Banerjee, and K. Thamilmaran, Chaos **27**, 013104 (2017).
[22] D. Premraj, K. Suresh, J. Palanivel, and K. Thamilmaran, Commun. Nonlin. Sci. Numer. Simulat. **50**, 103 (2017).
[23] A. Pikovsky, M. Rosenblum, and J. Kurths, *Synchronization: A Universal Concept in Nonlinear Sciences* (Cambridge University Press, Cambridge, 2001).
[24] Y. Kuramoto and D. Battogtokh, Nonlinear Phenom. Complex Syst. **5**, 380 (2002).
[25] A. Zakharova, M. Kapeller, and E. Schöll, Phys. Rev. Lett. **112**, 154101 (2014).
[26] G. C. Sethia and A. Sen, Phys. Rev. Lett. **112**, 144101 (2014).
[27] B. K. Bera, D. Ghosh, and T. Banerjee, Phys. Rev. E **94**, 012215 (2016).
[28] Z. G. Nicolaou, H. Riecke, and A. E. Motter, Phys. Rev. Lett. **119**, 244101 (2017).
[29] A. Goldbeter, *Biochemical Oscillations and Biological Rhythms* (Cambridge University Press, Cambridge, 1996).
[30] Y. Suzuki, M. Lu, E. B. Jacob, and J. N. Onuchic, Nat. Sci. Rep. **6**, 21037 (2016).
[31] E. Schöll, G. Hiller, P. Hövel, and M. A. Dahlem, Philos. Trans. R. Soc. London, Ser. A **367**, 1079 (2009).